POLITECNICO DI TORINO
Repository ISTITUZIONALE

WORKSPACE AND STABILITY ANALYSIS OF A MOBILE ELEVATING WORK PLATFORM USING
MULTIBODY DYNAMICS

(Article begins on next page)

01 September 2025

WORKSPACE AND STABILITY ANALYSIS OF A MOBILE ELEVATING WORK PLATFORM USING MULTIBODY DYNAMICS

Jnanashekar Prakash Reddy*   Giovanni Imberti*   Henrique de Carvalho Pinheiro*   Massimiliana Carello*

* Politecnico di Torino, DIMEAS, c.so Duca degli Abruzzi 24, Torino, 10129, Italy

ABSTRACT

Abstract: In this paper a Mobile Elevating Work Platform (MEWP) is modelled using Multi-Body Dynamics (MBD) to analyze its stability and find a safe workspace considering various external conditions like: wind load, weights in the basket and dynamic loads. The model considers the components of the MEWP as rigid, joints as ideal and disregards the dynamics and parasitic loads of the actuators. The contact forces between the outriggers/stabilizers and the ground have been considered in the model because are important for the stability control of the MEWP and they have been realized using Kelvin–Voigt spring-damper contact model. As stability of the MEWP depends on the outriggers position, a comprehensive study of stability in 3D space has been performed in different outrigger positions and finally the safe workspace is estimated.

Keywords: Multi-body Dynamics, Workspace Analysis, Ground contact modelling, Forward Kinematics.

1 INTRODUCTION

Mobile Elevating Work Platform Vehicles are equipped with telescopic platforms mounted on trucks as shown in Figure 1. MEWPs are widely used in various industries such as construction, maintenance, and repair. They provide easy and efficient access to elevated work areas, such as buildings, bridges, and industrial facilities. The goal of the MEWP is to have vehicles capable of reaching a wider operative space so that it could be possible to reduce the on-ground movement and, therefore, the operators' working times [1]. The main goal of this paper is to optimize the computational strategy for the evaluation of the safe workspace to precisely define the limit of the working area considering the normative limitations [2].

The stability of the MEWP is primarily determined by factors such as:
- position of its center of gravity,
- mass of the load in the basket,
- configuration of the outriggers,
- magnitude of external loads [3].

Contact author: Massimiliana Carello[1]

[1]Politecnico di Torino, DIMEAS, c.so Duca degli Abruzzi 24, Torino, 10129, Italy
 E-mail: massimiliana.carello@polito.it

The four outriggers can be extended, positioned, and fixed in various positions to suit the work environment.
 It is crucial to identify safe workspaces for the MEWP that consider different mass classes of the load in the basket and different configurations of the outriggers, and the external loads such as wind force, dynamic forces.

In literature it is possible to find different researches analyzing the stability of MEWPs [4], crane machines [5] and other similar systems [6], considering the computation of the stability around the axes created by the ground contact points generally extended for augmenting the safety operative domain and the outriggers.

The research on Mobile cranes [7] is a good starting point for the evaluation of the stability of this research that, although, has been overcome, using the Multibody dynamics approach [8, 9], for studying the stability and workspace of the MEWP. To reduce the computational time and cost, the components of the MEWP are considered rigid and the joints between the components are considered ideal while disregarding the friction [10, 11]. The inputs of the actuators are considered ideal, and their dynamics are neglected.

The goal of the paper is to develop a novel design tool capable of defining the operative limit of MEWPs starting from their geometrical characteristics. The control stability is evaluated considering the forces acting on each component, ensuring to consider also the regulatory forces described by the standard reference UNI EN [2].

In particular, the regulatory forces taken into consideration are:

- Wind Extra Force: computed considering a fixed coefficient to be multiplied to the variable aerodynamic forces' dependent on the operating surface. Only the forces significant for the stability evaluation have been taken into consideration.
- Operation Force: all the forces coming from the motions and operations of the workers inside the basket of the MEWP are considered and assumed to be acting only in the direction of gravity.
- Dynamic Forces: When the MEWP's components are rotating or extending, the inertial forces must be considered.

Figure 1 Mobile elevated work platform vehicles.

In this paper, MathWorks' Simscape Multibody is used to develop the multibody dynamics of the MEWP. The geometry of the components of the MEWP is modelled in Solidworks and imported in Simscape environment. MathWorks' MATLAB is used to postprocess the results from the MBD model and to plot 3D workspace. The results from the MBD model are compared with the equilibrium model which is presented in section 4. The results from the MBD model can be used to understand the limitations of the MEWP in terms of basket reach and corresponding pressure

values in the hydraulic piston are useful to develop control strategy to stabilize the MEWP. Pressure values of the hydraulic piston for both safe and unsafe operation of the vehicle are recorded, and the vehicle is operated under a certain threshold pressure which is always safe.

2 MULTIBODY MODELLING

2.1 MAIN COMPONENTS OF THE MEWP

A schematic diagram of the MEWP's chassis resting on the ground is shown in Figure 3 (a). The vehicle chassis is supported by 4 outriggers, 2 on the front and 2 on the rear. The bottom of the turret is connected to the chassis through a slewing ring and at the top it is connected to the boom casing through a revolute joint. The boom assembly is supported by a hydraulic piston which in turn connects to the turret. The boom casing houses 4 telescopic booms which are connected through prismatic joints as shown in Figure 2(b). The basket is mounted at the end of the 4th telescopic boom arm through a revolute joint which allows the basket to be constantly kept horizontal throughout its operation. The mass and dimensions of the components are reported in Table I. The MEWP consists of 3 main actuators which the 3D coordinates of the basket depend on. One at the turret and chassis revolute joint allows rotation of the turret in the global z-axis. A linear actuator in the hydraulic piston allows rotation of the boom casing and one more linear actuator in the telescopic boom enables extension of the boom. The outrigger's length can be extended according to the workplace conditions and the x-y coordinates of 4 possible cases are listed in Table II and shown in Figure 3 (b). In Case 1, all outriggers are extended completely and in Case 2, all outriggers are fully retracted. While in Case 3, the left outriggers are contracted fully and the right outriggers are extended to their maximum limit and in Case 4, the front outriggers are contracted fully, and the rear outriggers are extended completely.
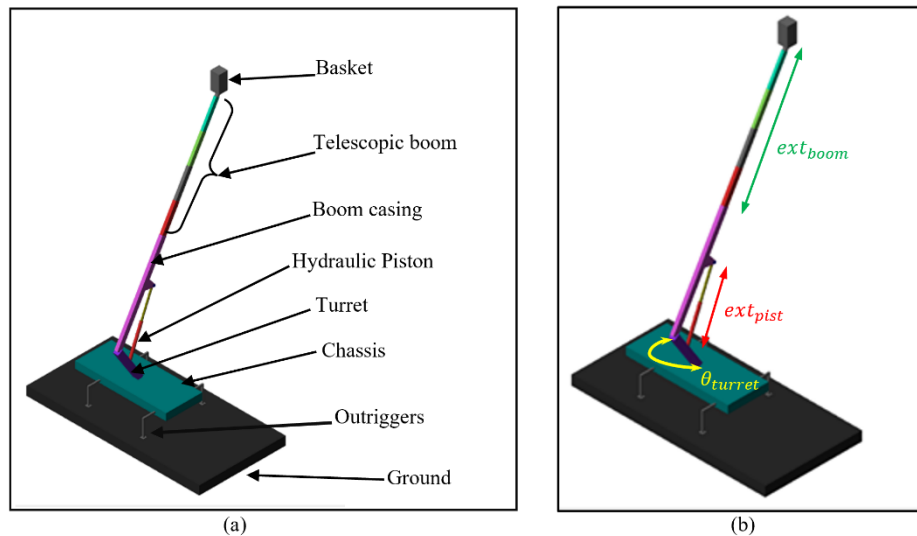

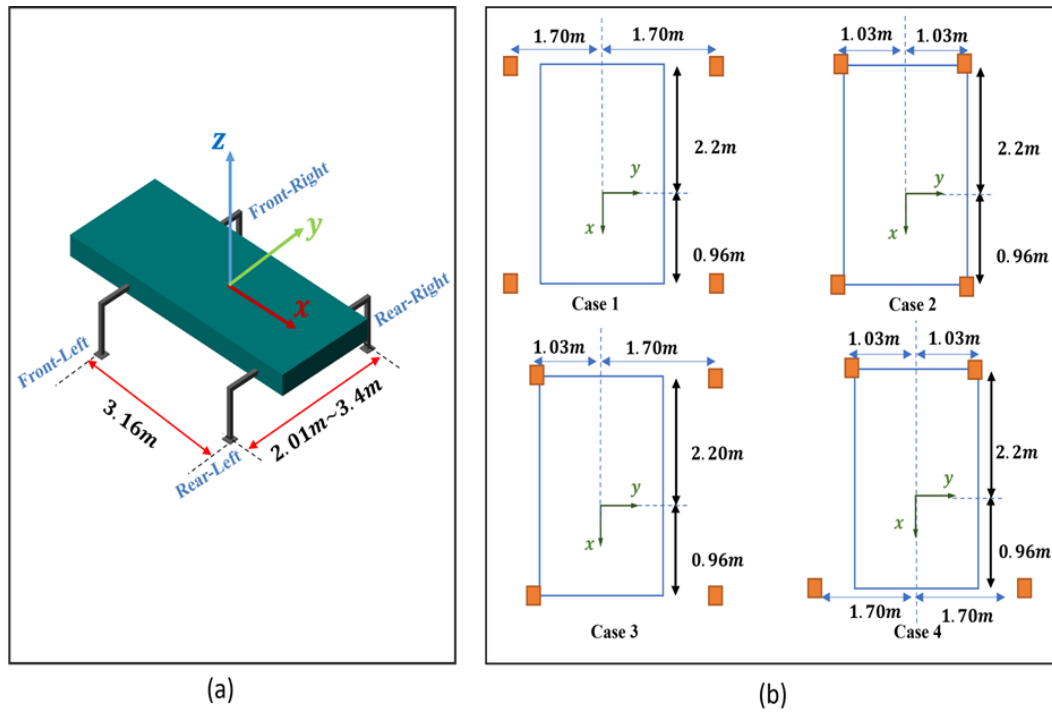Figure 2 (a) Scheme of the MEWP, (b) actuators of the MEWP.

Figure 3 (a) Coordinate system and (b) different outrigger positions of the MEWP.
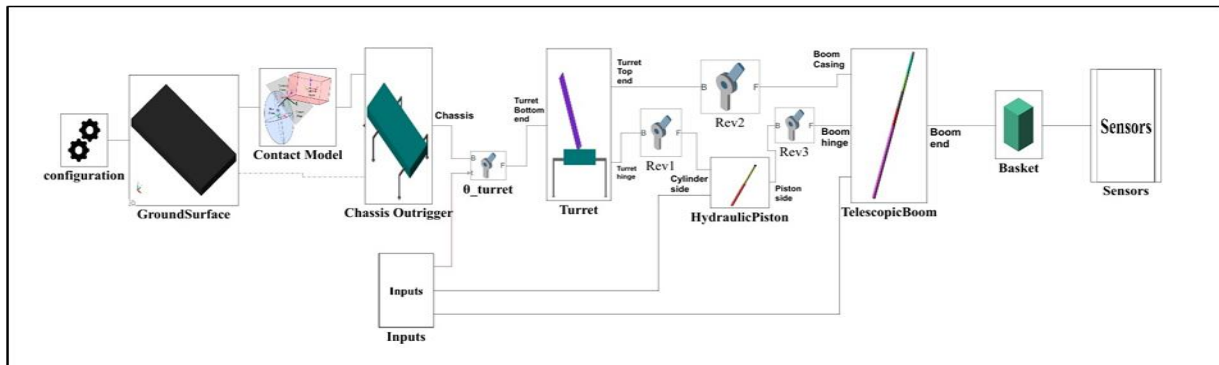

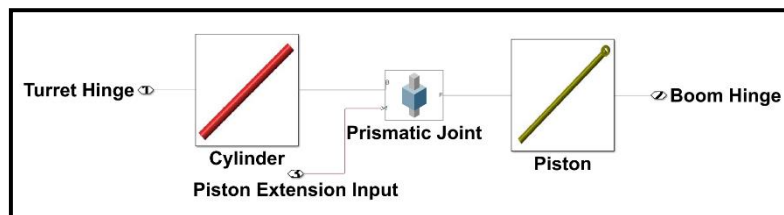Figure 4 MBD model of the MEWP in Simscape Multibody.

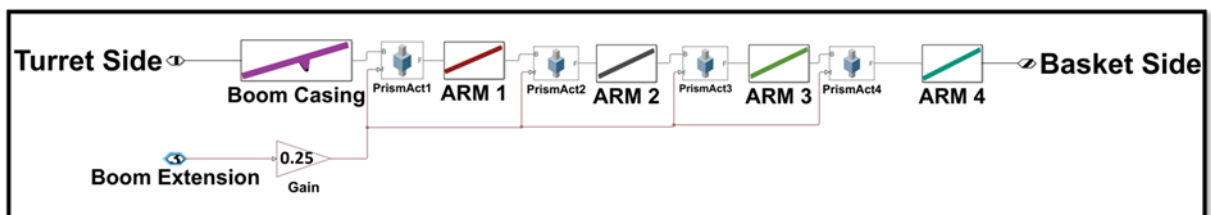Figure 5 MBD model of the hydraulic piston cylinder in Simulink.

Figure 6 MBD model of the Telescopic Boom in Simulink.

Table I - MEWP component mass and geometrical parameters

Components	Mass [kg]	Length [m]	Width [m]	Breadth [m]
Vehicle Body	2341	5.25	2.1	0.4
Turret	300	2.23	0.3	0.3
Boom Casing	254	5.221	0.26	0.19
Boom Arm 1	164	5.061	0.24	0.17
Boom Arm 2	103	5.018	0.23	0.16
Boom Arm 3	61	4.967	0.22	0.15
Boom Arm 4	48	4.967	0.21	0.14
Basket	45	1.2	0.7	0.7
Additional mass	0/80/250	0.2	0.2	0.2

Table II - Outrigger position coordinates in local coordinate system of the vehicle chassis (with reference to Figure 3(b))

Case	Front-Left [m]	Front-Right [m]	Rear-Left [m]	Rear-Right [m]
1	[0.96,-1.70,-1]	[0.96,1.70,-1]	[-2.2,-1.70,-1]	[-2.2,1.70,-1]
2	[0.96,-1.03,-1]	[0.96,1.03,-1]	[-2.2,-1.03,-1]	[-2.2,1.03,-1]
3	[0.96,-1.03,-1]	[0.96,1.70,-1]	[-2.2,-1.03,-1]	[-2.2,1.70,-1]
4	[0.96,-1.03,-1]	[0.96,1.03,-1]	[-2.2,-1.70,-1]	[-2.2,1.70,-1]

3 SIMSCAPE MULTIBODY MODEL OF THE MEWP

MBD model of the MEWP is developed in Simscape Multibody software and its scheme is shown in Figure 4. The model is created using Multibody library, where users can find body elements, joints, reference frames, and transforms etc. These individual blocks are parameterized and linked together in Simulink environment.

To create mechanisms with moving parts, body elements are linked through joints like prismatic, revolute, spherical joints etc., which allows bodies to move relative to each other.

The configuration block contains a world frame reference block and a solver configuration block which solves relative motions and calculates dynamic loads on the bodies and joints. A variable step (Simscape exclusive solver daessc) is used to solve the differential algebraic equations of the physical systems.

Various rigid components of the MEWP like chassis, turret, boom, piston, basket. are connected to each other through ideal joints and actuators. Some joints in this model are dependent, i.e., their motion/displacement is determined by the motion of the actuators. For instance, the rotation of the joints Rev1, Rev2 and Rev3 depends on the extension of the hydraulic piston depicted in Figure 4.

The cylinder and the piston are connected through a linear prismatic joint as shown in Figure 5. The telescopic boom is modelled by connecting individual arms through prismatic actuators as shown in Figure 6. The inputs for the actuators are smooth ramp signals which are saturated to specified values based on the forward kinematics.

The ground and the outriggers are connected through a spatial force block which computes contact reaction forces. The coordinates of the basket are measured and stored in the sensor block which will be used in post-processing to obtain the 3D workspace.

4 OUTRIGGER-GROUND CONTACT MODEL

The stability of the MEWP depends on the reaction forces exerted by the ground on the outriggers. Shyr-Long et al [12] analyzed the stability of the MEWP by finding the rection forces considering equilibrium of various loads at the center of gravity. Eq (1) shows the relation between the reaction forces and the loads on the MEWP.

$$
\begin{bmatrix} 1 & 1 & 1 & 1 \\ x_{R_1} & x_{R_2} & x_{R_3} & x_{R_4} \\ y_{R_1} & y_{R_2} & y_{R_3} & y_{R_4} \end{bmatrix} \begin{bmatrix} R_{1,z} \\ R_{2,z} \\ R_{3,z} \\ R_{4,z} \end{bmatrix} = \begin{bmatrix} F_{all,z} \\ M_{all,y} \\ M_{all,x} \end{bmatrix} \tag{1}
$$

where:
- $F_{all,z}$ is total weight of the vehicle and other forces in vertical direction,
- $M_{all,y}$ and $M_{all,x}$ are moment acting at the center of the vehicle along y axis and x axis respectively,
- $R_{i,z}$ is the reaction force on the ith outrigger,
- x_{R_i} and y_{R_i} are the distance between the ith outrigger and the center of gravity in x and y direction respectively.
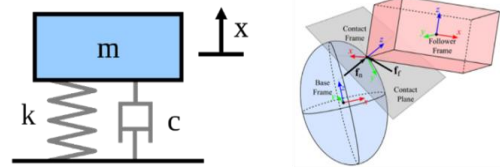

Figure 7 Ground contact force model (left) and Simscape model (right).

Newton's third law states that when two bodies are in contact, they exert equal and opposite force on each other, and the frictional force between them can be calculated using Coulomb's law. When two bodies are in contact with each other, as shown in Figure 7(left), the normal force acts along the point of contact and the frictional force acts perpendicular to the normal force and is in a plane contact plane.
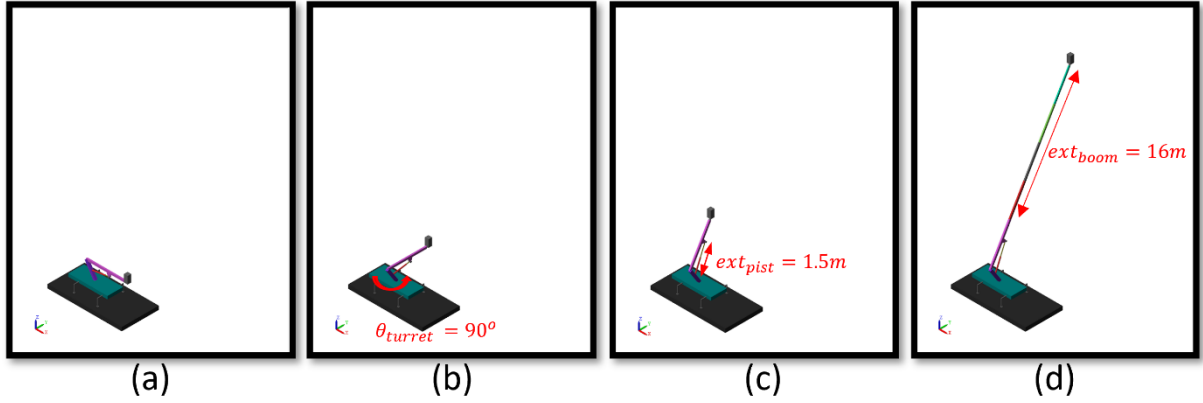
Figure 8 Sequence of operation of MEWP for actuator (parameter listed in Table IV).
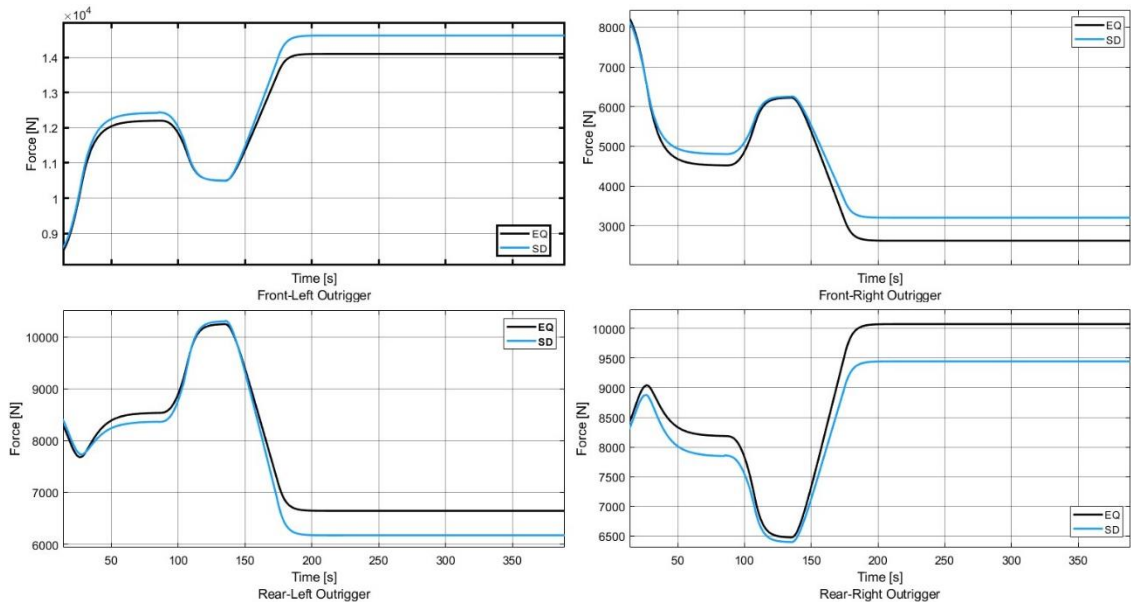

Figure 9 Comparison of reaction forces at outriggers calculated based on spring-damper and equilibrium.

Contact model developed by Kelvin–Voigt [12, 13, 14] is employed to find the outrigger-ground contact forces and is compared with the outrigger forces obtained by method presented by Shy-Long et al. [12].

The model considers spring damper system to find the contact forces as shown in Figure 7 (Right) [15] and the equation (2). The Kelvin–Voigt model is non-linear, but it is linearized by considering the spring and damper linear i.e. spring constant and damping co-efficient are constant. 4 spring-damper systems on each outrigger and a total of 16 systems are used to model contact between the outriggers and the ground.

In Simscape Multibody software, this can be realized using a spatial contact force block. This block applies a normal load to the bodies when the penetration depth (d) between them is less than the transition region width (w) specified, and the force applied is a linear function of the penetration depth. The normal force (f_n) varies linearly from zero to a maximum force based on Eq (2) [16, 17, 18, 19, 20].

The frictional force (f_f) is determined using Coulomb's law of friction as shown in Eq (3).

$$f_n = s(d, w) \cdot (k \cdot d + c \cdot d') \qquad (2)$$

Where: (f_n) is normal force, k is the spring constant, c is the damping coefficient, d is the penetration depth, d' is the first derivative of the penetration depth, $s(d, w)$ is the smoothing curve.

The force law is smoothed near the onset of penetration [21]. When $d < w$, the smoothing function increases continuously and monotonically over the interval $[0, w]$. The function, $s(d, w)$ is 0 when $d = 0$ and is 1 when $d = w$, and the function has zero derivative with respect to d at the endpoints of the interval. [22, 23].

$$f_f = \mu \cdot f_n \qquad (3)$$

Where f_f is the friction force, and μ is the static friction coefficient. A penetration depth of 1 mm is chosen which is small enough to depict the contact and big enough to have faster simulation and based on Eq (2) and Eq (3) corresponding spring constant, damping coefficient and coefficient of static friction values are calculated and are listed in Table III.

Table III - Contact model parameters

Penetration depth *(d)*	$1x10^{-3}\ m$
Spring constant (k)	$3.3x10^7\ N/m$
Damping coefficient (c)	$2.17x10^6 Ns/m$
Coefficient of static friction (μ)	0.5

Table IV - MEWP operation actuator parameters

Actuator parameter	Symbol	Value
Turret Rotation	θ_{turret}	90° (ACW)
Hydraulic piston extension	ext_{pist}	1.5 m
Telescopic boom extension	ext_{boom}	16 m

Table V - MEWP actuator parameters

Actuator parameters	Symbol	Min	Max	Interval
Turret Rotation	θ_{turret}	0°	360°	$0:3:360$
Hydraulic piston extension	ext_{pist}	$0\ m$	$1.8\ m$	$0:0.06:1.8$
Telescopic boom extension	ext_{boom}	$0\ m$	$16\ m$	$0:0.533:16$

Operation sequence of the MEWP is depicted in the Figure 8 for an arbitrary actuators' values (listed in Table IV) for which the MEWP is stable. The MEWP in the initial stage is shown in Figure 8 (a), the turret rotates 90° in anti-clockwise direction around its z axis to reach the position as shown in Figure 8 (b).

Then the piston rod extends to 1.5 m, which allows the boom to swing to a value of 60° with respect to horizonal plane as shown in Figure 8 (c). Finally, the telescopic boom extends fully to 1 6m bringing the basket to its final position as show in Figure 8 (d).

The outriggers' reaction forces are calculated using spring damper systems are compared with the reaction force calculated based on the equilibrium in the Figure 9. The forces calculated using two methods are comparable and the observed difference between two models can be attributed to two different states of the vehicle: dynamic and steady state. In the dynamic state, i.e., when the actuators are operating, the error is due to the inertia forces considered in the MBD model, which are ignored in the equilibrium model.

In the steady state, i.e., when the vehicle is at rest or the actuators are not operating, the error arises because the Kelvin-Voigt model is linearized.

Furthermore, it performs well at higher velocities of impact between bodies [14]. However, when the relative velocity is null between ground-outriggers, the model predicts forces that deviate from the correct values. Nevertheless, the error is minimal and is acceptable for this study.

5 SIMULATION RESULTS

To plot a safe 3D workspace, the stability of the MEWP should be analyzed at various positions of the basket in a 3D space. The position of the basket depends on the actuator parameters, so, they are divided into small intervals for better

resolution as shown in Table V. The MEWP is analyzed for 4 different outriggers as shown in Figure 3 (b) and corresponding positions in local co-ordinate system are reported in Table II.

5.1 TOP VIEW
Figure 10 shows top view of safe workspace of the MEWP for three different loads in the basket: 0, 80, and 250 kg. In Figure 10 (a), the reach of the MEWP is symmetric in the y-axis (width) and is maximum for 0 kg and reduces for 80 kg and 250 kg. For Case 2 of the outriggers shown in Figure 10 (b), reach reduces significantly. For Case 3 of the outriggers shown in Figure 10 (c), the reach is asymmetric along the y-axis and its magnitude is more in the right side than the left direction.

For Case 4, Figure 10 (d) of the position of the outriggers, the reach shape is like a curvy trapezium. In every case, the minimum reach of the MEWP is the same and is depicted by the black dotted line.

5.2 FRONT VIEW
The front view of the workspace of the MEWP is shown in Figure 11. The maximum basket reach in the z-axis is same in all cases while the reach along y-axis varies based on the outrigger position.

Like the top view, the reach for 0kg load in the basket is maximum and reduces as the mass increase to 80 kg and 250 kg. Figure 11 (a) shows the front view of the workspace for Case 1, the reach is symmetric and is maximum than any other case. For Case 2 shown in Figure 11 (b), the reach is symmetric like in Case 1, but the magnitude reduces significantly.

Reach of Case 3 depicted in Figure 11 (c) is not symmetric and is maximum on the right side. For Case 4, shown in Figure 11 (d), the reach is similar to Case 2.
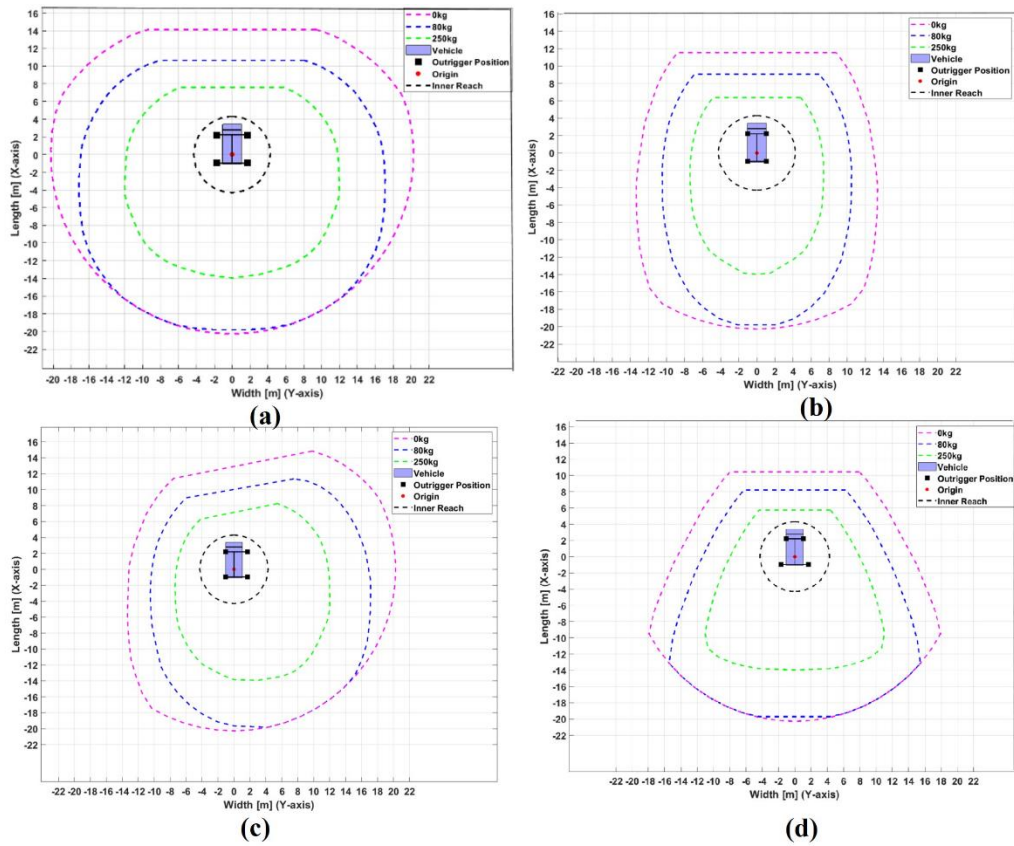
Figure 10 Top view of the workspace for various mass loads in the basket for outrigger position:
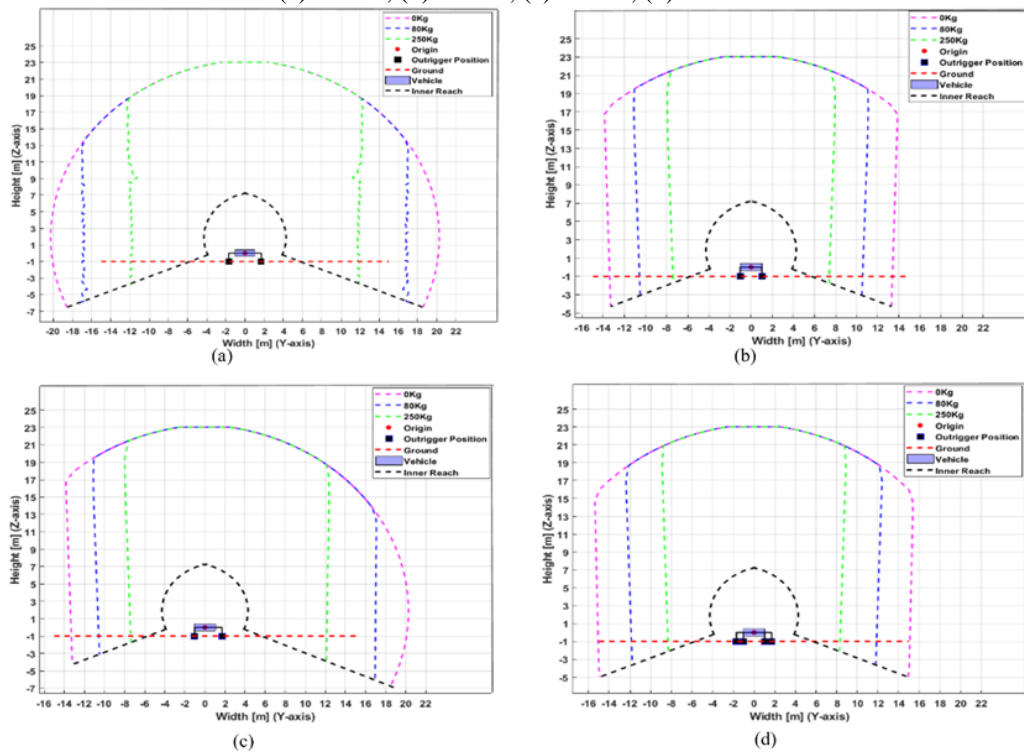(a) Case 1, (b) Case 2, (c) Case 3, (d) Case 4.

Figure 11 Front view of the workspace for various mass loads in the basket for outrigger position:
(a) Case 1, (b) Case 2, (c) Case 3, (d) Case 4.

5.3 SIDE VIEW

The reach in the side view is same for all the cases irrespective of the outrigger position case and is shown in Figure 12 . For the 0 kg load, reach is not symmetric in the side view. On the rear it has the maximum reach and is only restricted by the geometric reach. However, in the front, the reach is significantly less than the rear because of the instability and presence of the cab. The shape and magnitude of reach for the load class of 80 kg is almost similar to that of the load class 0 kg and in the front, the shape is similar, but the magnitude is significantly lower because of the instability. For the load class 250 kg, the shape and magnitude of the reach is restricted by the instability of the vehicle and is much lower than that of other load classes.
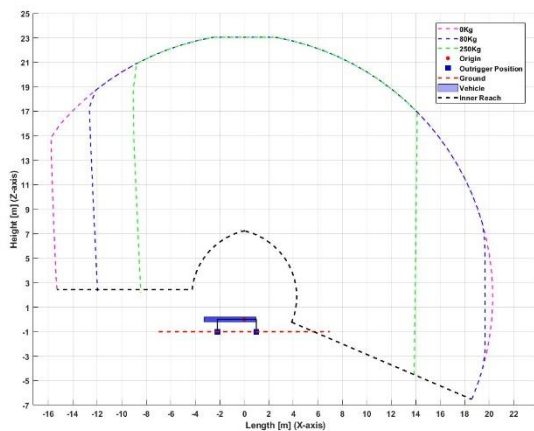

Figure 12 Side view of the workspace of various load classes for outrigger position.

2 CONCLUSIONS

In this paper, a multibody dynamics modelling has been developed to find a safe workspace of a Mobile Elevating Work Platform considering its components as rigid and joints and actuators as ideal. A simple linear mass spring damper system is employed to model the contact and find reaction forces between outriggers and the ground. A 360o stability analysis of the MEWP is performed to find a safe 3D workspace and the results are discussed. This model accurately depicts the dependency of MEWP's stability on its outriggers position. The results have also been compared to commercial company data for guaranteeing a reliable correlation between the model and the real MEWP behavior. Further the model developed is a modular multi-body tool which can evaluate the stability of a MEWP during the design phase. The tool has been modeled for ensuring the possibility of developing multiple studies, starting from the actual normative, but also adding other dependencies, such as the flexibility of the components or the case of impulsive loads falling from the basket. The above-mentioned cases are a critical aspect and, in the future, from a regulatory point of view, it will be important to take them into consideration, so that the MEWPs operation is safe for both operators and the environment around the vehicle.

REFERENCES

[1] C. S. Pan, A. Hoskin, M. McCann, M.-L. Lin, K. Fearn and P. Keane, "Aerial lift fall injuries: A surveillance and evaluation approach for targeting prevention activities," Journal of Safety Research, vol. 38, no. 6, doi.org/10.1016/j.jsr.2007.08.002, pp. 617-625, 2007.

[2] UNI EN 280:2013+A1:2015, Mobile elevating work platforms - Design calculations - Stability criteria - Construction - Safety - Examinations and tests., 2015.

[3] Crane safety - General Design, London: BSI Standards Publication, 2021.

[4] D. O. Aikhuele, "Evaluation of the root cause of failure in a crawler crane machine using hybrid mcdm model," Trans RINA, Vols. 161, Part A3, no. DOI: 10.3940/rina.ijme.2019.a3.523, pp. 219-228, 2019.

[5] W. Kacalak, M. Majewski and Z. Budniak, "Crane stability assessment method in the operating cycle," Transport Problem, vol. 12, no. 4, DOI:10.20858/tp.2017.12.4.14, pp. 141-151, 2017.

[6] W. Wolfslag, G. Xin, C. Tiseo and S. Vijayakumar, "Optimisation of Body-ground Contact for Augmenting Whole-Body Locomanipulation of Quadruped Robots," in 2020 IEEE/RSJ International Conference on Intelligent Robots and Systems (IROS), Las Vegas, NV, USA, 2020.

[7] S.-L. Jeng and W.-h. Chieng, "Outrigger Force Measure for Mobile Crane Safety Based on Linear Programming Optimization," Mechanics Based Design of Structures and Machines, vol. 38, no. 2, pp. 145-170, 2010.

[8] J. L. Dominique P. Chevallier, Multi-Body Kinematics and Dynamics with Lie Groups, London, UK: ISTE Press Ltd and Elsevier Ltd, 2018.

[9] J.Angeles and A. Kecskemethy, Kinematics and Dynamics of Multibody, Udine: Springer-Verlag Wien, 1995.

[10] M. Blundell and D. Harty, The Multibody systems approach to Vehicle Dynamics, Coventry, UK: Elsevier, 2015.

[11] H. de Carvalho Pinheiro, A. Messana, L. Sisca, A. Ferraris and A. G. A. &. M. Carello, "Computational Analysis of Body Stiffness Influence on the Dynamics of Light Commercial Vehicles," in Advances in Mechanism and Machine Science, Springer International Publishing, DOI: 10.1007/978-3-030-20131-9_307, 2019.

[12] D. Zhang and W. Whiten, "The calculation of contact forces between particles using spring and damping models," ELSEVIER, vol. 88, no. 1, DOI:10.1016/0032-5910(96)03104-X, pp. 59-64, 1996.

[13] M. S. S. &. J. McPhee, "Foot–ground contact modeling within human gait simulations: from Kelvin–Voigt to hyper-volumetric models," Multibody Syst Dyn, vol. 35, no. 1, DOI: 10.1007/s11044-015-9467-6, pp. 393-407, 2015.

[14] J. S. M. B. Luka Skrinjar, "A review of continuous contact-force models in multibody dynamics," International Journal of Mechanical Sciences, vol. 145, no. https://doi.org/10.1016/j.ijmecsci.2018.07.010, pp. 171-187, 2018.

[15] Matlab, "Spatial Contact Force," Mathworks, 2019. [Online]. Available: https://www.mathworks.com/help/sm/ref/spatialcontactforce.html. [Accessed 1 September 2022].

[16] F. F. S. Dubowsky, "Dynamic analysis of mechanical systems with clearances-Part 2: dynamic response," Journal of Engineering for Industry, vol. 93, no. 1, DOI: 10.1115/1.3427896, pp. 310-316, 1971.

[17] T. G. S. Dubowsky, "Design and analysis of multilink flexible mechanisms with multiple clearance connections.," J Eng Ind Trans ASME, vol. 99 Ser B, no. 1, https://doi.org/10.1115/1.3439171, pp. 88-96, 1977.

[18] J. D. S. D. T. Kakizaki, "Modeling the spatial dynamics of robotic manipulators with flexible links and joint clearances," J Mech Des, vol. 115, no. 4, DOI: 10.1115/1.2919277, pp. 839-847, 1993.

[19] A. S. Y.A. Khulief, "A continuous force model for the impact analysis of flexible multibody systems," Mech Mach Theory, vol. 22, no. 3, DOI: 10.1016/0094-114X(87)90004-8, pp. 213-224, 1987.

[20] L. J. a. Z. B. Fox, "Numerical computation of differential-Algebraic equations for non-Linear dynamics of multibody systems involving contact forces," J Mech Des, vol. 123, no. 2, DOI: 10.1115/1.1353587, p. 272, 2001.

[21] M. A. H. G. R. B. G. Rabbat, "Friction coeffcient of steel on concrete or grout," The Journal of Structural Engineer, vol. 111, no. 3, doi:10.1061/(asce)0733-9445(1985)111:3(505), pp. 505-515, 1984.

[22] A. Messana, A. Ferraris, A. G. Airale, A. Fasana and M. Carello, "Enhancing Vibration Reduction on Lightweight Lower Control Arm," Hindawi, Shock and Vibration, vol. 2020, no. DOI: 10.1155/2020/8891831, 2020.

[23] H. de Carvalho Pinheiro, A. Messana, M. Carello and N. and Rosso, "Multibody parameter estimation: a comprehensive case-study for an innovative rear suspension," in SAE International, https://doi.org/10.4271/2022-36-0059, 2022.